REDUCING MECHANICAL ANISOTROPY IN EXTRUSION-BASED PRINTED PARTS

Chad Duty[1,2], Jordan Failla[1,2], Seokpum Kim[1,2], John Lindahl[2], Brian Post[2], Lonnie Love[2], Vlastimil Kunc[1,2,3]

[1]University of Tennessee
[2]Manufacturing Demonstration Facility, Oak Ridge National Laboratory
[3]Purdue University

Abstract

The mechanical performance of 3D printed components is highly dependent upon the orientation of the part relative to the build plane. Specifically for extrusion-based printing systems, the bond between successive layers (z-direction) can be 10-25% weaker than in the printed plane (x-y plane). As advanced applications call for fiber reinforced materials and larger print systems (such as the Big Area Additive Manufacturing system) extend the layer time, mechanical performance in the z-direction can decrease by 75-90%. This paper presents a patent-pending approach for improving mechanical performance in the z-direction by depositing material vertically across multiple layers during the build. The "z-pinning" process involves aligning voids across multiple (n) layers, which are then back-filled in a continuous fashion during the deposition of layer (n+1). The "z-pinning" approach has been demonstrated to be an effective approach for increasing the strength (20% increase) and toughness (200% increase) of printed parts in the z-direction.

Background

The popularity of 3D printing has grown sharply in the last several years due primarily to the emergence of the desktop 3D printer, generically known as Fused Filament Fabrication (FFF). However, the utilization of FFF technology is largely restricted to the production of demonstration pieces, models, and prototypes that test only the form and fit of a given design. The functionality of a printed component is often limited by poor mechanical performance. Although engineering polymers, such as acrylonitrile butadiene styrene (ABS), are used for 3D printing applications, the component-level strength of a printed part can be a fraction (as low as 25-50%) of the cited reference strength for that material (typically from a compression or injection molded reference).

The relatively poor mechanical performance of FFF parts is largely due to manner in which material is deposited during the extrusion-based printing process. Although the technology is popularly referred to as "3D printing", the traditional approach to building a three dimensional geometry by successively stacking 2D layers of deposited material can more accurately described as "2.5-D printing". The layered structure of a traditionally-printed component is immediately apparent by close inspection of a given cross section (Figure 1). Using the conventional nomenclature where the deposition plane is the x-y plane and the z-axis is directed vertically across layers, it is evident that FFF printing can align continuous material in any specific direction within

the x-y plane, but there is no continuous material crossing between successive layers [1]. Therefore, transferring a load in the z-direction (vertically in Figure 1) must occur across the discrete bonded areas where the deposited beads in successive layers interact. At best, these bonded areas are intermittent across a given load path and are subject to stress concentrations due to the sharp interfaces where the curved surfaces of the beads intersect.

Figure 1. Cross section of an extrusion-based 3D printed part showing layered architecture.

In order to reduce mechanical anisotropy in the x-y plane, the majority of FFF printing approaches stagger the orientation of deposited material relative to the x- and y-axes in a cross-hatched (45/-45) manner. Previous studies [2] have shown that the mechanical strength of ABS samples can vary from a maximum of ~30 MPa when deposited beads were parallel to the load direction, to a minimum of ~5 MPa when they were oriented perpendicular to the load direction. A (45/-45) crosshatch in-fill pattern in the x-y plane was shown to improve the strength only slightly (~10 MPa) from the minimum value, but provides an attractive degree of homogeneity in the x-y plane. A similar trend was demonstrated for polylactic acid (PLA) samples in the same study [2], with a strength of ~55 MPa when parallel, ~30 MPa when perpendicular, and ~38 MPa using a (45/-45) crosshatch.

Torrado Perez et al [3] demonstrated that the strength in the z-direction of ABS samples printed on a MakerBot were ~50% weaker than corresponding samples printed in the x-y plane. The modulus of the samples tested in the z-direction did not drop as much (~22%), but the elongation to failure was dramatically reduced (4.5% in the x-y plane compared to 1.5% in the z-direction). Given the layered nature of traditional FFF printing, it's not feasible to use a (45/-45) crosshatch approach to homogenize strength in the z-direction, so a new approach is needed.

Z-Pinning Approach

The "z-pinning" approach (patent pending [4]) deposits continuous material across multiple layers in a 3D printed component, effectively stitching together the layered 2.5D structure in the third dimension (z-axis). As shown in Figure 2, the z-pinning process involves aligning voids across multiple (n) layers, which are then back-filled in a continuous fashion during the deposition of layer (n+1) or as a separate step between layers (n) and (n+1). As illustrated in Figure 2, the z-

pinning approach begins with leaving intentionally aligned voids or openings across (n) layers in the standard cross-hatch infill pattern of a printed component (n=4 in Figure 2a). Either during or prior to deposition of the following layer (n+1), the deposition head moves into position above the opening and remains stationary while extruding material to fill the void (Figure 2b). Note that additional openings are present in Figure 2b that will not be filled after layer (n) because they are the locations of pins that will be deposited in later steps. As noted, Figure 2c illustrates that as the printing process continues for additional layers, voids are aligned above the previously deposited pin as well as in neighboring locations for the placement of staggered pins. In this example of two pin locations, after deposition of layer (n + n/2) in Figure 2c, the deposition head is positioned over the alternate pin location and extrudes material (n) layers deep to fill the void (Figure 2d). Note that the x-y location of the pin deposited in Figure 2b remains open. After deposition of (2n) layers are complete with appropriately aligned voids, another z-pin is deposited in the original x-y location, penetrating (n) layers deep to bond with the previous pin (Figure 2e). The z-pinning process continues in Figure 2f for layer (2n + n/2) and proceeds accordingly through the thickness of the printed part.

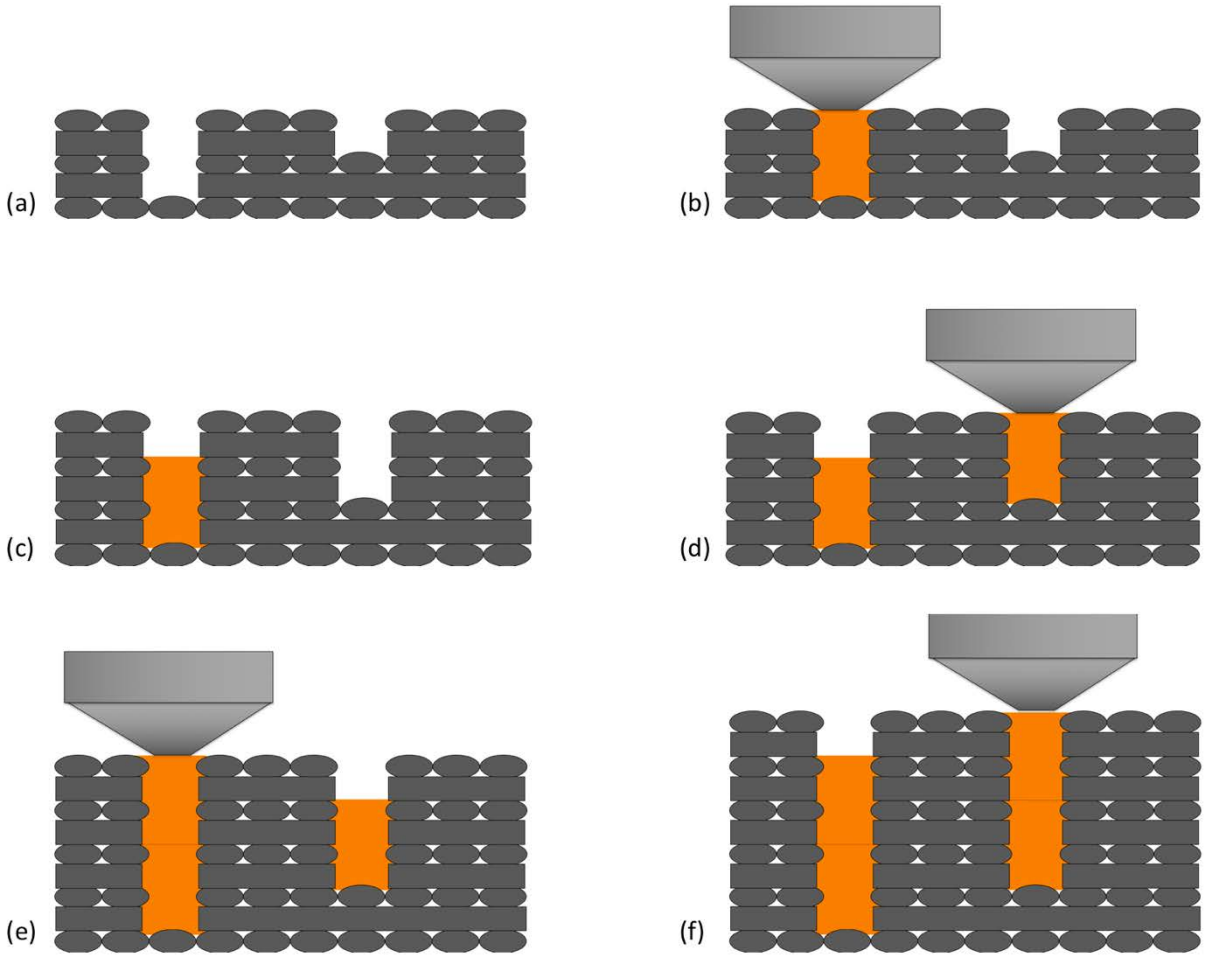

Figure 2. Z-Pinning approach for depositing continuous material across successive layers.

In addition to enabling continuous deposition of material between successive layers, the z-pinning approach has several advantages. The natural wall structure of stacked beads that form an intentional void in FFF printing is generally scalloped, with several periodic undulations and deep crevices. As the z-pin is extruded to fill the void, the hot extruded material can flow into these pockets and become mechanically interlocked with the surrounding structure, regardless of whether any traditional re-melt molecular bonding occurs. This may become especially important for printing with multiple materials (even across broad material categories such as thermoplastics, thermosets, ceramics, metals, composites, etc) that do not share common processing conditions that are suitable for bonding. As research continues in the area, the shape of aligned voids can be specifically designed to enhance mechanical interference between the pin and the layered structure. The z-pinning approach also offers a unique opportunity for fiber-reinforced materials. Since reinforcing fibers typically shear-align parallel to the extrusion flow direction, z-pinning is the only approach which allows these reinforcing fibers to align vertically and improve strength and stiffness in the z-direction.

The apparent weak point in a z-pinned structure is the bond (or seam) between successive pins. Assuming that the voids spaces completely fill and intimate contact is achieved between the pins, the resulting bond can be no better than the bond between successive layers in a traditional print. Therefore, for z-pinning to be effective, the seam between successive pins needs to be staggered within the bulk structure – similar to the mortar joints in a brick wall. The stagger pattern for seams depends on several factors, including the pin length (n) as measured in number of layers, the number of layers between pin deposits (i), and the spacing of pins in the x-y plane. The z-pin approach described in Figure 2 has a pin length of 4 layers (n=4) and pins are deposited in different holes every 2 layers (i=2). Note that the ratio of (n/i) must be an integer value in order for pins to be deposited continuously throughout the structure (ignoring seams). The nomenclature used in this study for printing with a pin length (n) and layer frequency (i) is “n-i pins”. For example, Figure 2 demonstrates the deposition of 4-2 pins.

The variation of x-y spacing and configurations are numerous and varied. For the purpose of this study, the standard in-fill pattern consisted of an orthogonal rectilinear grid in which all of the deposited beads in one layer were aligned along a primary axis (x-axis) and the beads of the following layer were aligned with the orthogonal axis (y-axis). This base grid pattern alternates throughout the part, leaving a grid of aligned voids throughout the structure. Z-pins were inserted at alternating locations across the x-y plane. The two spacing patterns utilized in this study are illustrated in Figure 3, where the A-B pattern utilizes an (n/i) ratio of two, and the A-B-C pattern utilizes an (n/i) ratio of three.

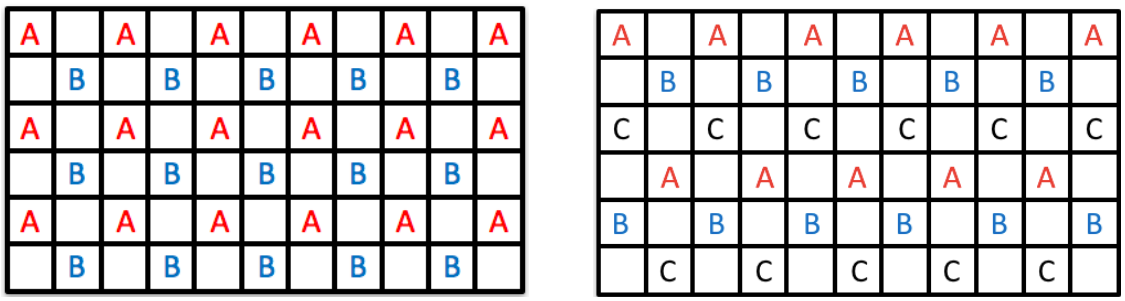

Figure 3. Pin spacing configuration in the x-y plane for A-B (left) and A-B-C (right).

The proper pin parameters for a given in-fill pattern can vary considerably depending upon the material and deposition system being used, as well as the desired performance for the intended application. The rectilinear grid pattern described above results in a square hole that is open on alternating sides for a given layer, similar to a log cabin layup, as shown in Figure 4a. The theoretical volume of the available hole can be calculated analytically, but the actual "fill volume" of a successfully deposited pin is typically below this theoretical limit. Additionally, the penetration depth of a single pin (n) must be identified for a given material and print system to insure that adequate contact with the underlying pin is made. Finally, the ratio between the diameter of the hole (D_h) to the diameter of the extrusion orifice (D_e) is critical. If the diameter ratio is too small, the pin will likely not penetrate the full distance (n) and an "overfill" condition will result. If the ratio is too large, the thin extruded material will accumulate loosely within the hole and not penetrate appropriately into the surrounding structure (like rope coiling in a bucket). Figure 4b shows a simple rectilinear grid without pins and Figure 4c demonstrates an appropriately pinned sample using A-B spacing. The pin conditions selected for the current study were a pin volume of 80% theoretical, a hole depth of 1.6-2.4 mm (n = 8-12 layers), and diameter ratio (D_h/D_e) of 3 (corresponding to D_h ~ 1mm). Figure 5 illustrates complete penetration of 8 layer pins made from black PLA in a rectilinear matrix of orange PLA. The mechanical interlocking of the pins with the surrounding structure is apparent.

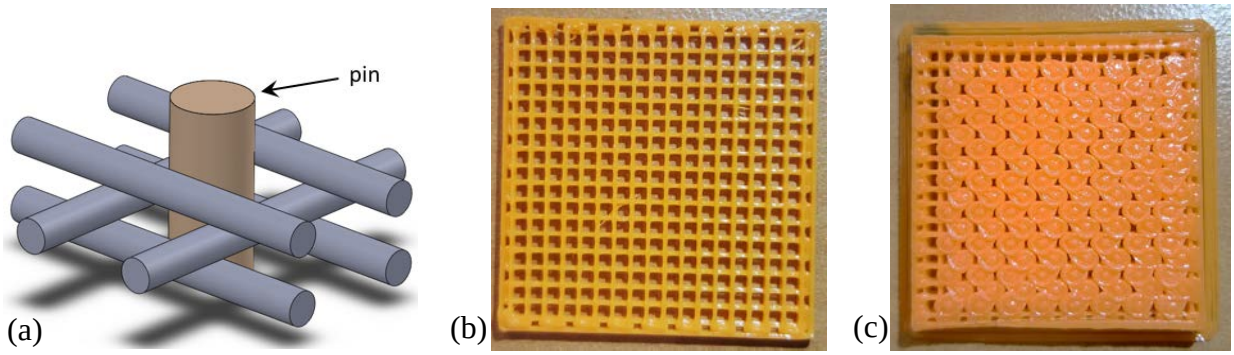

Figure 4. Illustration (a) of a rectilinear grid system without z-pins (b) and with A-B z-pins (c).

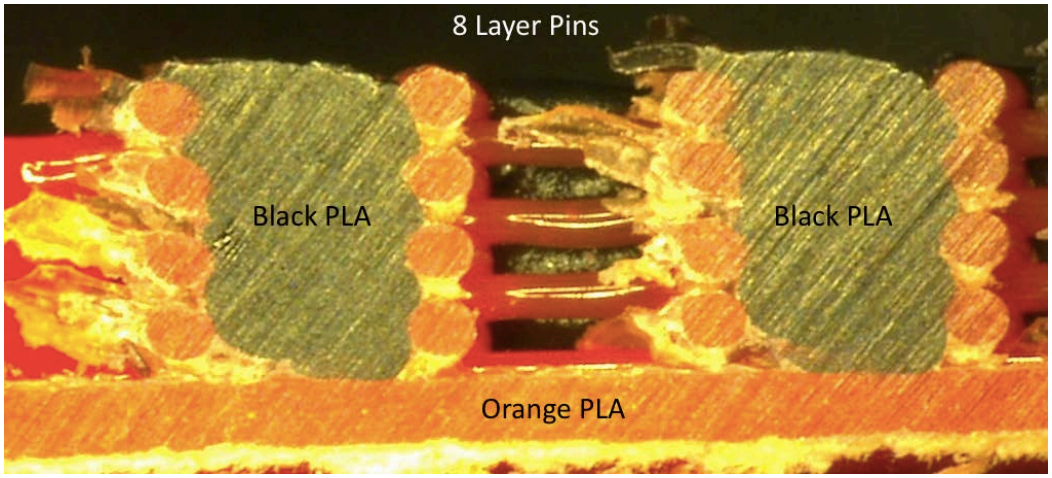

Figure 5. PLA Z-pins (black) of length (n=8) in a PLA (orange) grid structure.

Experimental Procedure

In order to evaluate the mechanical performance of z-pinned materials, tensile specimens printed on a MakerGear M2. The machine code for the desktop printer was customized to generate the rectilinear grid pattern described previously in the x-y plane. Samples were either printed without pins (NP) or with pins using the A-B or A-B-C spacing pattern from Figure 3. An 35% in-fill pattern was found to provide the appropriate hole diameter and grid spacing needed for the deposition of successful pins. A rectilinear grid using a 57% in-fill was also printed without pins to represent a "constant-mass" control (i.e. having the same mass as the 35% in-fill samples that contained z-pins). The MakerGear M2 used a 0.35 mm nozzle with a layer height of 0.20 mm. The material was standard PLA filament feedstock purchased from 3DXTech and was deposited a nominal temperature of 220°C. A variation on the z-pinning approach involved the deposition of "hot pins" where the rectilinear grid structure was deposited at the nominal temperature of 220C, but extrusion of the z-pins occurred at 240C. The motivation behind the "hot pin" concept was to increase the bonding temperature with the surrounding structure as well as reduce the viscosity of the pinning material to improve penetration into the surrounding geometry. Note that the z-pinning process described here requires only software modifications to the printing system, meaning that this technique can be utilized on virtually any open-source desktop FFF or extrusion-based printer.

The geometry of the tensile samples designed specifically for this study is shown in Figure 6. The upper and lower grip sections of the samples were built with a 100% solid infill through the transition regions. The rectilinear grid section measured 25 mm x 13 mm in cross section and did not use a solid outer contour. This allowed each pinned sample to contain 68 pins across the x-y plane. The grid section extended 35 mm in the build direction (z-axis), containing ~175 layers. The tensile samples were tested using a MTS Series 40 Electromechanical Universal Test System with a 100 kN load cell at a strain rate of 5 mm/min. Engineering stress was calculated based on a nominal apparent cross section of 25 mm x 13 mm and strain measurements were taken from the machine crosshead displacement. All tensile samples (at least 4 samples for each condition) printed with neat PLA failed in the grid gauge section, well away from the solid transition regions.

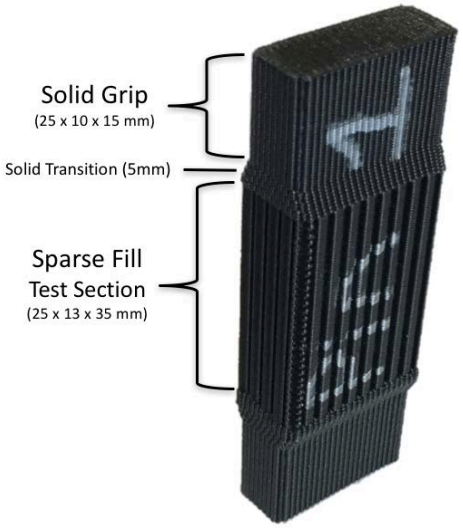

Figure 6. Z-pin tensile sample geometry.

Experimental Results & Discussion

Figure 7 compares the tensile properties of a 35% infill sample with 12-6 z-pins against a control sample without pins. The pinned sample demonstrates a slightly higher ultimate tensile strength (20% increase) and a dramatically improved toughness (100% increase). The strain to failure for the z-pinned sample increased by more than 60% and the stiffness of the samples were nearly identical.

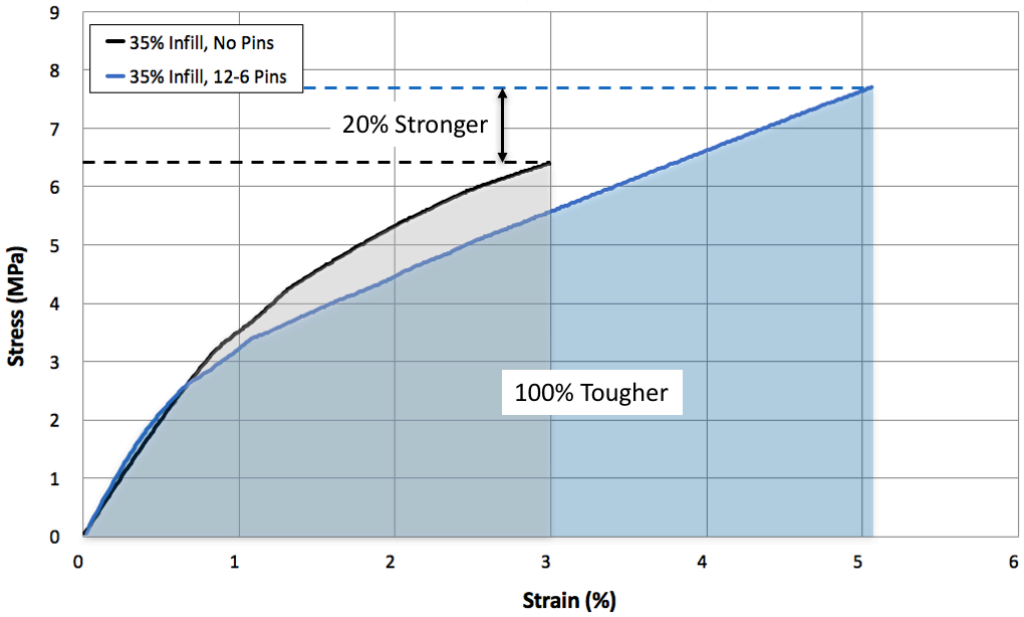

Figure 7. Tensile test of 35% infill sample without (black) and with (blue) z-pins.

The ultimate tensile strength across the variety of samples printed is compiled in Figure 8. The first two samples demonstrate the expected reduction in strength for un-pinned 35% infill samples loaded in the z-direction as compared to the x-y plane (~60% reduction). The second sample (35% infill, no pins) serves as the baseline for evaluating the effectiveness of a variety of pin configurations. The 8-4 and 12-6 pin configurations both show a statistically significant improvement in tensile strength compared to the un-pinned sample (~20% increase). The samples printed with 12-4 pins demonstrated a slight increase (~10%), but it is estimated that the higher frequency of pausing the print to insert pins resulted in a higher number of defects and poorer bonding between successive layers. The 57% infill pattern without pins resulted in a significantly higher tensile strength than any of the 35% infill samples tested in the z-direction. On a per-mass basis, the 35% infill samples that contained pins were equivalent to the un-pinned 57% infill samples, but the strength of the 57% infill sample was significantly higher (~60%) than any of the pinned samples and almost twice as high as the un-pinned 35% infill samples. This indicates that for the same mass using the current pin printing configuration for neat PLA, improved strength can be attained by increasing the density of the infill pattern rather than inserting z-pins. However, further optimization of the pin configuration (e.g. pin volume, diameter ratio, penetration depth, stagger pattern, etc) may likely reverse this trend. For instance, using a “hot pin” approach, where the deposition temperature of the z-pin was increased by 20°C, resulted in an additional 10% increase in tensile strength.

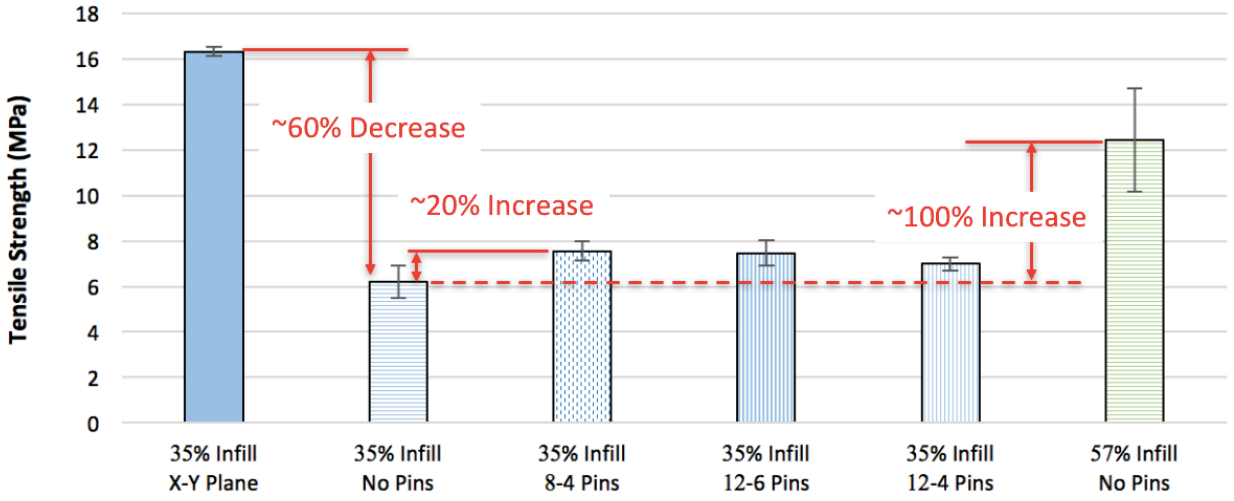

Figure 8. Ultimate strength of z-pin samples compared to control samples (4 samples each).

A similar trend can be observed in the measured toughness of the printed samples in Figure 9. The reduction in toughness due to print direction is dramatic (~90% reduction in the z-direction). As illustrated in Figure 7, the 12-6 pinned sample doubled the toughness in the z-direction, but the toughness of the 57% infill samples without pins was still far superior.

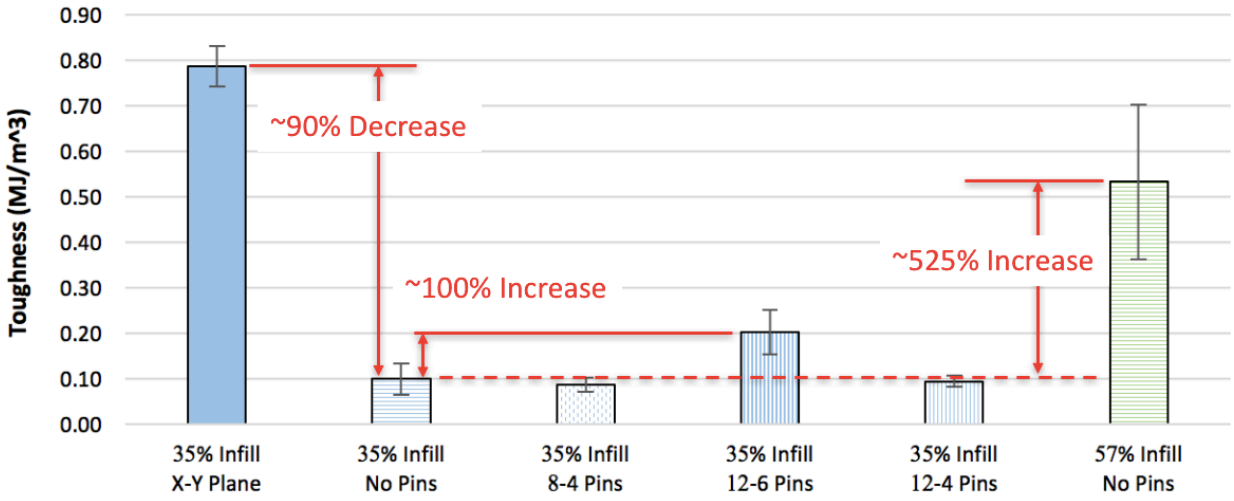

Figure 9. Toughness of z-pin samples compared to control samples (4 samples each).

Inspection of the fracture surfaces of the tensile samples (Figure 10) shows a distinct difference in the exposed surface area. The samples without pins (35% and 57% infill) have a relatively smooth fracture surface, indicating that the crack in the specimen likely propagated across a single layer (or layer interface) in the x-y plane with very little deflection. The pinned samples, regardless of configuration, resulted in a very tortuous fracture surface, indicating that the crack was deflected several times as it worked across the specimen's cross section.

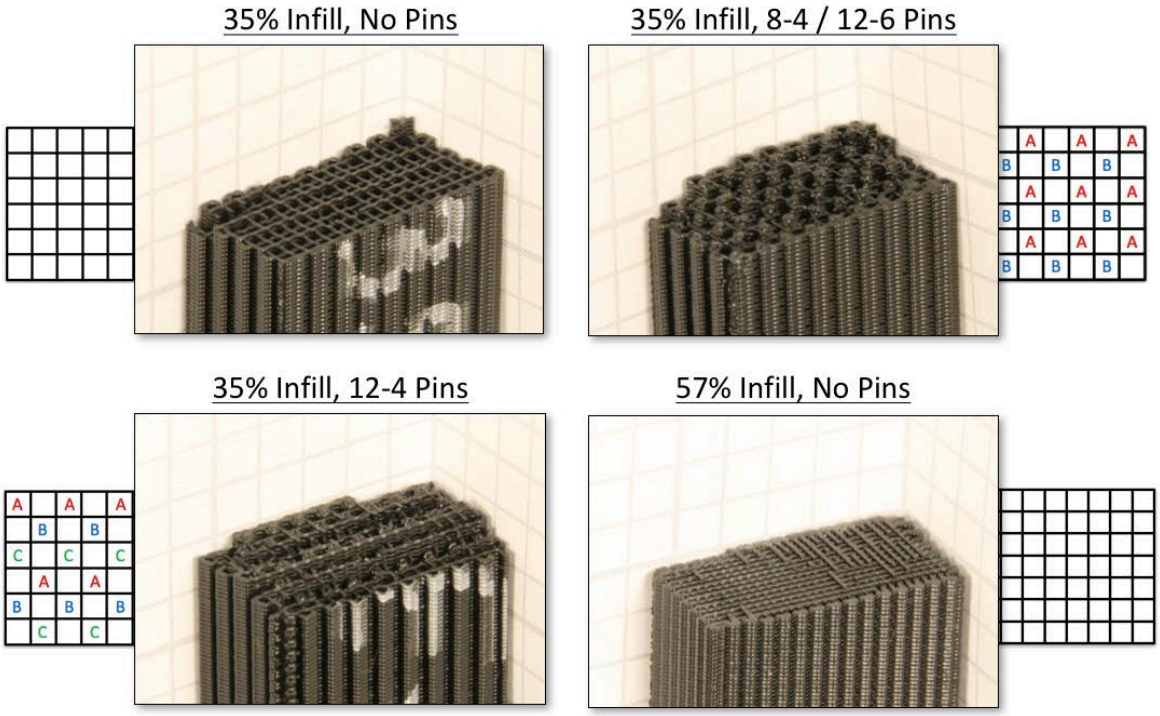

Figure 10. Fracture surface of representative tensile specimens.

The crack deflection behavior can be seen more directly in Figure 11, in which the crack clearly deflects to re-route the path between embedded pins (locations highlighted in red). The additional energy absorbed by the structure is evident in damage created parallel to the load direction as the crack path traverses across multiple layers. It can be observed that the crack deflects a specific number of layers in each case that matches the pin length (n=12). As expected, this identifies the bond between successive pins as the weak link, but can provide guidance on further configurations to improve both strength and toughness.

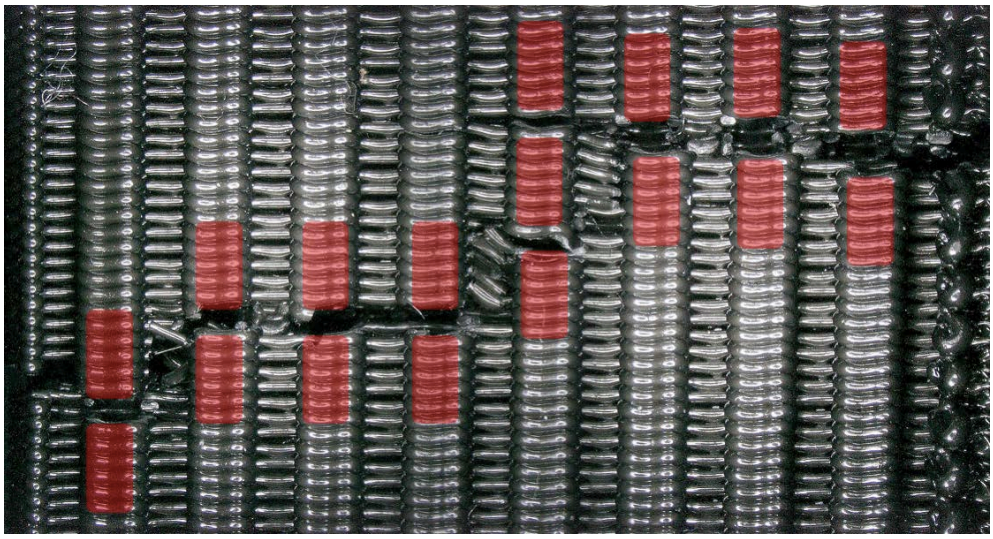

Figure 11. Fracture path of 35% infill, 12-6 pin sample with pin locations highlighted.

Conclusions & Future Work

A novel z-pinning approach has been described for 3D printing which allows for continuous deposition of material across successive layers within the bulk of a printed part. The z-pinning approach has wide application for fiber reinforced materials, joining of dissimilar materials, and is appropriate across a broad spectrum of extrusion-based platforms. Initial studies with carbon fiber reinforced PLA has shown promise for exceeding the strength of even 57% infill control samples, and the z-pinning concept has also been demonstrated on large scale systems like Big Area Additive Manufacturing (BAAM). Since the z-pinning approach requires only software modifications to existing open-platform printers, it is susceptible to wide-scale adoption across the 3D printing industry. Much work remains to optimize pinning conditions for various materials and print platforms, but the approach shows great promise.

Acknowledgements

A portion of the research was sponsored by the U.S. Department of Energy, Office of Energy Efficiency and Renewable Energy, Advanced Manufacturing Office, under contract DE-AC05-00OR22725 with UT-Battelle, LLC.

References

[1] Bellini, A. and S. Guceri. (2003) "Mechanical Characterization of Parts Fabricated Using Fused Deposition Modeling." *Rapid Prototyping Journal* **9** (4).

[2] Shaffer, S., K. Yang, J. Vargas, M. Di-Prima, and W. Voit. (2014) "On Reducing Anisotropy in 3d Printed Polymers Via Ionizing Radiation." *Polymer* **55**: p. 5969-5979.

[3] Torrado-Perez, A., D. Roberson, and R. Wicker. (2014) "Fracture Surface Analysis of 3d-Printed Tensile Specimens of Novel Abs-Based Materials." *Journal of Failure Analysis and Prevention* **14**: p. 343-353.

[4] Duty, C., J. Failla, V. Kunc, J. Lindahl, B. Post, L. Love, and S. Kim (2017) "Z Layer Improvement Using Liquid Nails Method." U.S. Patent Application 62/491,313 filed April 28, 2017.